2008

# Functional characterization of alternatively spliced human SECISBP2 transcript variants

Laura V. Papp, *Queensland Institute of Medical Research*
Junning Wang, *University of Massachusetts Medical School Worcester*
Derek Kennedy, *Griffith University*
Didier Boucher, *Queensland Institute of Medical Research*
Yan Zhang, *University of Nebraska - Lincoln*, et al.

*7192–7206* *Nucleic Acids Research, 2008, Vol. 36, No. 22* *Published online 12 November 2008*
*doi:10.1093/nar/gkn829*

# Functional characterization of alternatively spliced human *SECISBP2* transcript variants

**Laura V. Papp[1], Junning Wang[2], Derek Kennedy[3], Didier Boucher[1], Yan Zhang[4], Vadim N. Gladyshev[4], Ravindra N. Singh[2] and Kum Kum Khanna[1,*]**

[1]Signal Transduction Laboratory, Queensland Institute of Medical Research, 300 Herston Rd, 4029 Herston, Queensland, Australia, [2]Department of Medicine, University of Massachusetts Medical School, Worcester, MA 01605, USA, [3]School of Biomolecular and Biomedical Science, Eskitis Institute for Cell and Molecular Therapies, Griffith University, 4111 Nathan, Queensland, Australia and [4]Department of Biochemistry and Redox Biology Center, University of Nebraska, Lincoln NE 68588, USA

Received July 10, 2008; Revised October 10, 2008; Accepted October 14, 2008



## ABSTRACT

**Synthesis of selenoproteins depends on decoding of the UGA stop codon as the amino acid selenocysteine (Sec). This process requires the presence of a Sec insertion sequence element (SECIS) in the 3′-untranslated region of selenoprotein mRNAs and its interaction with the SECIS binding protein 2 (SBP2). In humans, mutations in the SBP2-encoding gene Sec insertion sequence binding protein 2 (*SECISBP2*) that alter the amino acid sequence or cause splicing defects lead to abnormal thyroid hormone metabolism. Herein, we present the first *in silico* and *in vivo* functional characterization of alternative splicing of *SECISBP2*. We report a complex splicing pattern in the 5′-region of human *SECISBP2*, wherein at least eight splice variants encode five isoforms with varying N-terminal sequence. One of the isoforms, mtSBP2, contains a mitochondrial targeting sequence and localizes to mitochondria. Using a minigene-based *in vivo* splicing assay we characterized the splicing efficiency of several alternative transcripts, and show that the splicing event that creates mtSBP2 can be modulated by antisense oligonucleotides. Moreover, we show that full-length SBP2 and some alternatively spliced variants are subject to a coordinated transcriptional and translational regulation in response to ultraviolet type A irradiation-induced stress. Overall, our data broadens the functional scope of a housekeeping protein essential to selenium metabolism.**

## INTRODUCTION

Selenocysteine (Sec), the 21st amino acid in the genetic code, is incorporated into a subset of proteins termed selenoproteins in response to an in-frame UGA codon (1). Since the UGA codon most commonly signals translation termination, its decoding as Sec relies on the presence of several unique, evolutionary conserved structures and protein factors. The major *cis*-acting determinant for Sec incorporation is the Sec insertion sequence (SECIS) element, a stem–loop RNA structure located within the 3′-untranslated region (UTR) of all eukaryotic selenoprotein mRNAs (2,3). This element acts by recruiting the specialized protein complexes required for the read-through of UGA and translation of selenoproteins. An additional RNA structure able to support UGA codon read-through, named the Sec redefinition element (SRE), has been recently identified within the coding region of selenoprotein N, a few nucleotides downstream of the UGA codon (4). While the SECIS element is absolutely required for Sec incorporation, the SRE appears to play only a fine-tuning role in determining the UGA decoding efficiency for some selenoproteins (5). Synthesis, delivery and incorporation of Sec into polypeptide chains is supported by selenocysteyl-tRNA$^{[Ser]Sec}$(1) and by a set of specialized proteins [reviewed in (6)], including SECIS binding protein 2 (SBP2) (7,8), Sec-specific elongation factor eEFSec (9,10), ribosomal protein L30 (11),

*To whom correspondence should be addressed. Tel: +61 7 3362 0338; Email: kumkumK@qimr.edu.au
Correspondence may also be addressed to Laura V. Papp. Tel: +61 7 3845 3738; Email: Laurap@qimr.edu.au
Present addresses:
Junning Wang, Harvard Medical School-Partners Healthcare Center for Genetics and Genomics (HPCGG), New Research Building, Room 164, 77 Avenue Louis Pasteur, Boston MA 02115.
Ravindra N. Singh, Department of Biomedical Sciences, College of Veterinary Medicine, Iowa State University, Ames, IA 50011, USA

the 43 kDa RNA binding protein (SECp43) and Sec synthase (12). Although much progress has been made in delineating individual components required for selenoprotein synthesis, the overall mechanism that directs this process is not fully understood.

SBP2 is one of the most studied selenoprotein synthesis factors, initially shown to be required for this process in reticulocyte lysates and *in vitro* assays (8,13). Consistent with this, we have shown that SBP2 depletion in human cells leads to decreased selenoprotein synthesis (14). Hereafter, we refer to SBP2 as protein, whereas Sec insertion sequence binding protein 2 (*SECISBP2*) in italicized letters refers to gene or transcript. The first *in vivo* evidence showing that SBP2 is epistatic to selenoprotein synthesis was recently provided in a study that identified mutations in *SECISBP2* in families presenting with clinical evidence of abnormal thyroid hormone metabolism (15). This was manifested through lack of functional selenoenzyme deiodinase 2 (DIO2) and dramatically reduced levels of selenoprotein P in affected individuals (15). Detailed biochemical and functional characterization of SBP2 has been carried out; however, its regulation at the gene and transcript level requires further studies.

Alternative splicing represents a functionally important and a major regulatory pathway of gene expression and ultimately protein function. Recent genomic studies have indicated that at least 60% of mammalian genes are subjected to alternative splicing (16), providing a significant contribution to protein diversity beyond that encoded in the genome sequence. Most alternative splicing events affect the coding sequence and it is believed that half of these alter the reading frame (17), and a third lead to nonsense mediated decay (NMD) of the RNA product (18). Defects in alternative splicing and generation of aberrant ratios of mRNA transcripts from a single gene are now also recognized as major contributors to human disease and it is estimated that at least 15% of the mutations that cause hereditary disease affect pre-mRNA splicing (19). Splicing defects have also been associated with cancers and a genome wide analysis of human expressed sequence tags (ESTs) found strong evidence for cancer specific splice variants in 316 human genes (20–24). To date, this level of regulation has not been explored for any of the factors involved in Sec incorporation, including SBP2.

SBP2 is the only protein of the Sec incorporation machinery so far linked to a clinical condition (15). Interestingly, one of the mutations identified in patients alters the splicing of *SECISBP2* by creating an alternative donor splice site, which produces a transcript with a 26 bp intron retention. This event alters the reading frame upstream of the SBP2 RNA-binding domain, giving rise to a truncated, non-functional protein. The regulation of SBP2 expression by alternative splicing thus appears to have significant implications for its function. Prompted by these findings, we herein carried out *in silico*, as well as functional analysis of alternative splicing of *SECISBP2*. We now provide evidence for a complex alternative splicing pattern in the 5′-region of human *SECISBP2* that give rise to eight spliced variants generated through different exon combinations. All alternative splicing events are confined within the region of SBP2 that is dispensable for Sec incorporation *in vitro*, but may be involved in regulation of selenoprotein synthesis *in vivo*. Interestingly, one of the alternatively spliced isoforms contains a mitochondrial targeting sequence (MTS). We designated this transcript as mitochondrial Sec insertion sequence binding protein 2 (*mtSECISBP2*). First, using a minigene-based *in vivo* splicing assay we delineated the splicing events within the 5′-region of *SECISBP2* and showed that splicing of *mtSECISBP2* can be modulated by antisense oligonucleotides (ASOs). We furthermore demonstrated that the protein encoded by *mtSECISBP2* does indeed localize to mitochondria and that transcription and translation of SBP2 is regulated in a coordinated manner in response to stress.

## MATERIALS AND METHODS

### *In silico* identification of alternatively spliced forms of SBP2

The previously characterized human full-length *SECISBP2* gene (GeneBank ID: NM_024077) was used to search against both the EST and the non-redundant (NR) nucleotide databases to identify alternative forms of human *SECISBP2* gene. Sequence analyses were performed using BLAST programs (available at http://www.ncbi.nlm.nih.gov/BLAST/) with default parameters. Tissue- and cell-type information of various ESTs was also retrieved from EST database. Identified sequences that were homologous to *SECISBP2* were then mapped to human genomic sequences to analyze genomic structures of detected alternative forms. Cellular localizations of proteins were predicted by PSORT II (http://psort.ims.u-tokyo.ac.jp/form2.html).

### Cell culture and treatments

The cell lines human embryonic kidney 293T, human cervical carcinoma C33A, human cervical carcinoma HeLa and normal foreskin fibroblast (NFF) cells, were maintained in RPMI 1640 medium supplemented with 10% fetal calf serum (Gibco-BRL, Gaithersburg, MD, USA) and 1% penicillin/streptomycin, in a humidified atmosphere containing 5% $CO_2$. For Ultraviolet A (UVA) treatments, media was removed and kept at 37°C, and phosphate buffered saline (PBS) was added. Cells were subjected to a dose of 50 kJ/m$^2$ of UVA irradiation. Control cells were maintained in PBS at room temperature, in the dark, for the duration of treatment. Following irradiation, the PBS was replaced with the media and cells were allowed to recover for the time indicated.

### Generation of minigenes

*SECISBP2* minigene splicing cassette was generated by amplifying genomic sequences starting from exon 1 through exon 4 of the *SECISBP2* gene with high-fidelity *Pfx* polymerase (Invitrogen, Carlsbad, CA, USA) and genomic DNA (Clontech Laboratories, Inc. Palo Alto, CA, USA). Appropriate primers were used to reduce the size of intron 2 from ~5.6 kb to 356 nt that include 184 residues of the 5′-end of intron 2 and 172 residues of the

3′-end of intron 2. An ~2.3 kb amplified fragment from genomic *SECISBP2* containing entire exon 1, entire intron 1, entire exon 2, partial intron 2 (only 356 nt), entire exon 3, entire intron 3 and entire exon 4 was cloned into pCI vector (Promega) between Xho I and Not I site. Subsequently, genomic sequences from the pCI vector were subcloned into a SBP2-GFP plasmid described previously (14). Here, appropriate primers were used to replace exon 1 through exon 4 of SBP2 cDNA sequence with ~2.3 kb genomic sequence described above (Figure 2A). The complete SBP2 minigene sequence is provided as supplementary data. Mutations were introduced using the Quick-Change site directed mutagenesis kit (Stratagene) as per manufacturer's instructions.

### Antisense oligonucleotides

ASOs were synthesized by Dharmacon, Inc. The sequences of the oligonucleotides used are as follows: mG(*)mA(*)mU(*)mC(*)mG(*)mA(*)mU(*)mC(*)mG(*) mA(*)mU(*)mC(*)mG(*)mA(*)mU(*)mC(*)mG(*)mA(*) mU(*)mC(*)mG(*)mA for the control ASO (GATC) and mC*mU*mG*mC*mC*mU*mA*mA*mG*mU*mA*mA* mA*mA*mA*mG*mU*mG*mU*mA*mA*mA*mC for the SBP2 specific ASO spanning the intron 2-exon 3a boundary (In2E3a). In these sequences, the letter m represents an *O*-methyl modification at the second position of a sugar residue and an asterisk represents a phosphorothioate modification of the backbone.

### Transfections and *in vivo* splicing assays

All reagents were used according to the manufacturer's recommendations. Transient transfections of cells with plasmid DNA or antisense oligonucleotides were performed with Lipofectamine 2000 (Invitrogen). Cells were plated into 6-well plates 24 h prior to transfection so that their density on the day of transfection was 70%. 2.0 μg of plasmid DNA was used per well. For co-transfection experiments, cells were transfected with 1.0 μg of plasmid DNA and 100 nM of ASO per well. Total RNA was isolated 24 h after transfection with Trizol reagent (Invitrogen). To generate cDNA, reverse transcription was carried out with a SuperScript II reaction kit (Invitrogen) using oligo(dT) primer. Generally, 1.0 μg of total RNA was used per 20 μl of reaction mixture. Minigene-specific spliced products were subsequently amplified with forward primer annealing in the vector sequence (P1GFP) 5′-GCTAGCGCATCCGGACTCA GAT-3′, and the reverse SBP2-specific primer annealing in exon3b 5′-CTTAAACAGAGCTTTCATTTCTTGTG G-3′ using *Taq* polymerase (Invitrogen). Analysis and quantifications of spliced products were performed with an FPL-5000 Image Reader and ImageGauge software (Fuji Photo Film Inc.) Results were confirmed by three independent experiments.

### Expression of endogenous *SECISBP2* transcripts

For analysis of endogenous full-length *SECISBP2* and *mtSECISBP2*, C33A, HeLa and 239T cells were transfected with 100 nM ASOs per well of a 6-well dish. Total RNA was isolated 24 h after transfection with the RNeasy Mini Kit (Qiagen). Reverse transcription was carried out with oligo (dT) primers and SuperScript II (Invitrogen) as described above. Full-length *SECISBP2* and *mtSECISBP2* transcripts were subsequently amplified by real-time RT-PCR with transcript-specific forward primers 5′-TCCTTATACCCTTGACTCCACA-3′ for full-length *SECISBP2* and 5′-CCAGTGACAGAAATG TTTACTCAG-3′ for *mtSECISBP2*, and the same reverse primer 5′-TCCTGTCTGTTCGCTTATGG-3′. Glyceraldehyde 3-phosphate dehydrogenase (GAPDH) was used as an internal standard (Fwd 5′-CTGCACACCAAC TGCTTAG-3′; Rev 5′-GTCTTCTGGGTGGCAGTG AT-3′). Real-time RT-PCR was performed using Platinum SYBR Green qPCR SuperMix-UDG (Invitrogen) in a Rotor-Gene 6000 (Corbett Life Science) according to the instructions provided with the kit. Cycling conditions were used as suggested in the SYBR Green kit instructions. Results were analyzed using relative quantification software (Corbett Life Science).

### Cell lysis and western blotting

Cells were lyzed in universal immunoprecipitation buffer (UIP) as described previously (14). Proteins were separated on 4–12% gradient gels (Invitrogen) unless otherwise stated. Western blotting was performed using the following antibodies: anti-SBP2 and anti-HSP70 antibodies raised in house as described previously (14), anti-actin (Sigma), anti-GFP (Molecular Probes, Invitrogen) and anti-SBP2 antibodies (EC1) (Everest Biotech, Oxfordshire, UK). Except for Figure 4B, images were acquired using an LAS-3000 luminescent image analyzer (Fujifilm Life Science, Stanford, CT, USA). The western blot in Figure 4B was developed using traditional X-ray film.

### Fluorescence microscopy

Cells, untransfected or transfected with GFP-tagged proteins, were washed in PBS twice and fixed with 4% paraformaldehyde in PBS for 30 min at room temperature. 4′,6′-Diamidino-2-phenylindole (DAPI) was used to stain the nuclei and MitoTracker CMXRos (Molecular Probes, Invitrogen) (50 nM) was used to stain mitochondria. For immunofluorescence, coverslips were blocked in 3% horse serum in PBS, incubated with anti-SBP2 antibody (EC1) at 1 : 250 dilution, followed by incubation with an Alexa fluor 488 dye-conjugated secondary antibody (Molecular Probes, Invitrogen). Colocalization of SBP2 with mitochondria was detected using a double immunofluorescent procedure. Coverslips were mounted with ProLong Gold (Molecular Probes, Invitrogen). Images were acquired in 20 z-sections by using a state-of-the art DeltaVision PD system microscope (Applied Precision, Washington, USA) with a 60× or 100× objective. Images were subsequently deconvolved with 10 cycles of the DeltaVision PD software.

## RESULTS

### Human SBP2 is alternatively spliced

In humans, the *SECISBP2* gene spans a 43 kb region on chromosome 9q22.1 and consists of 17 exons.

Following reverse transcription PCR (RT-PCR) of the 5′-end of *SECISBP2* using mRNA isolated from 293T cells, we observed a second PCR product, shorter than the full-length transcript (data not shown). Sequence analysis of this band identified two alternatively spliced *SECISBP2* variants: one lacking exon 2, and the second lacking part of exon 3, further designated exon 3a. To further examine whether additional *SECISBP2* splice variants were present in humans, we searched EST and NR databases using known full-length *SECISBP2* sequences and mapped and quantified the identified cDNAs onto the genomic sequence. This search confirmed that full-length *SECISBP2* is indeed the most abundant transcript, currently represented by ~120 ESTs and 5 complete mRNAs, and led to the identification of seven alternatively spliced *SECISBP2* variants arising through different exon combinations. These variants are as listed in Table 1 along with their proposed nomenclature. A schematic representation of the genomic organization of human *SECISBP2* is shown in Figure 1A, and the spliced variants for which sufficient sequence was available to determine their complete 5′-exon combination are presented in Figure 1B. The three functional domains of SBP2: the RNA binding domain, the Sec insertion domain and the ribosome interacting domain, are located within the C-terminal part of the protein (8,25), which corresponds to exons 12–16. Interestingly, all alternative splicing events occur upstream of exon 11, within the region dispensable for Sec insertion *in vitro*.

Sequence analysis of exon/intron boundaries showed that nearly all splice sites within the 5′-region of *SECISBP2* conform to consensus sequences (AAG|GU or CAG|GU at the 5′-exon/intron boundary and CAG|G at the 3′-end) (26) with only a few deviations (Table 2). The majority of exons have one donor and one acceptor splice site; however, exons 3 and 7 have multiple acceptor sites, denoted as a, b, c or d. A very complex splicing pattern was noted between exons 6 and 7, with four possible splicing combinations. The most common acceptor site was the 7a site. The 6–7b splice variant appeared to be rare, however, an encoding mRNA derived from brain tissue (Table 1) was present in the EST database. The variants 6–7c and 6–7d were covered by several ESTs.

All *SECISBP2* transcripts for which sufficient 5′-sequence information was available appear to begin with exon 1. This suggests the usage of a common promoter, located upstream of exon 1. As mentioned above, the overwhelming majority of *SECISBP2* transcripts include all exons. However, the alternatively spliced *SECISBP2* variants seem to be expressed in normal as well as in cancer-derived tissues (Table 1). The best represented alternatively spliced transcript lacked exon 3a as evidenced by 24 ESTs from normal and cancer-derived tissues and cell lines, and was also covered by three complete mRNAs (Table 1). Despite the presence of a large number of ESTs covering the 5′-region of *SECISBP2* sequence, no alternative splicing events were detected downstream of exon 10.

### Alternative splicing of *SECISBP2* creates several open reading frames

We next examined the nucleotide sequences of the various transcripts for their potential to encode complete open reading frames (ORFs), and found that five SBP2 isoforms initiating from five different ATG start sites can be encoded (Figure 1C). As previously shown, the full-length SBP2 is translated using the first ATG codon in exon 1. This main ORF is however abrogated for some of the variants as premature termination codons (PTCs) are generated, suggesting a possibility of the use of alternative ATG start sites. As indicated in Figure 1B, these potential alternative translation initiation sites (referred by amino acid numbering in full-length SBP2) are methionine (Met) 69 within exon 3a for SBP2_Δ2, and Met 233 within exon 5 for SBP2_Δ3 and they are in the same frame as full-length SBP2. However, for the *mtSECISBP2* and *SECISBP2E6* transcripts, the first ATG codon downstream of the PTC is created in a different frame in exon 2 (Met 33) and in exon 6 (Met 283) respectively (Figure 1B). These reading frames create a short N-terminal amino acid composition different to full-length SBP2 (i.e., 27 aa for mtSBP2 MVRVLRSMCLP QLCSHILSVCSGTTSDR, and 11 aa for SBP2E6 MP LPILLHVQE), however, these reconnect with the full-length SBP2 reading frame at the next splice site. Interestingly, motif analysis using the PSORTII program predicted the existence of a classical MTS within the exon 3a-deleted variant (Figure 1C), and this form is further designated as mitochondrial SBP2, mtSBP2. The alternate reading frame for SBP2E6 did not seem to encode any targeting signals or motifs different to full-length SBP2. The complex splicing pattern between exon 6 and 7 was interesting as all splicing variations lead to changes in the amino acid composition of the encoded proteins. The splicing from exon 6–7c and 6–7d lead to deletion of a stretch of 38 or 39 amino acids (aa 294–331 or aa 294–332) from exon 7 ($^{294}$ELSWTPMGYVVRQTLSTELSAAPKNVTS MINLKTIASS$^{331}$), however, the reading frame starting in exon 1 is maintained throughout both isoforms. The ESTs covering the *SECISBP2_Δ9* transcript did not have sufficient sequence upstream of the splicing event in order to determine its translation initiation sites; however, ORF prediction indicated that the reading frame in exon 1 can be maintained despite exon 9 skipping.

### Evolutionary aspects of splicing events within SBP2

We next investigated the extent of alternative splicing events in SBP2 in other species. We thus analyzed the distribution of *SECISBP2* homologs, the conservation of splicing events and evolution of the *SECISBP2* gene in genomic and EST databases. As recently established, selenoprotein genes are widely distributed among eukaryotes including all vertebrates and most arthropods, nematodes, protozoa and lower plants (27–29). Selenoproteins were lost in fungi, land plants, some insects and most eukaryotic parasites. We found that *SECISBP2* homologs are present in all selenoprotein-containing genomes, and absent in EST and genomic databases of organisms lacking Sec utilization, suggesting that *SECISBP2* co-evolved

**Table 1.** Alternatively spliced human *SECISBP2* transcripts

| Transcript name | Exon combination | No. of ESTs | Normal tissue or cell line | Primary tumors | Cancer derived or transformed cell lines | Complete mRNAs |
|---|---|---|---|---|---|---|
| *SECISBP2* | 1–17 | ~120 | Present in most tissues | Present in several tumors | Present in several cell lines | NM024077<br>AK090608<br>AX746532<br>BC036109<br>AF380995 |
| *mtSECISBP2* | 1,2–3b,4,5,6 ... | 24 | Pooled glandular (CB956376)<br>Pancreas (BM315064)<br>ES cell lines (CN256608, CN256604, CX870404)<br>T-lympnocytes (CR994587)<br>Liver Cho-CK cell line (CB121625)<br>Thymus (DB160135)<br>Small intestine (DA926236)<br>Fetal brain (DA803510)<br>Thalamus (DA403753)<br>Corpus callosum (DA283160)<br>Testis (DB459197, DC399547)<br>Pooled mixed tissue (CV029893) | Retinoblastoma (BE252177)<br>Choriocarcinoma (BG481218)<br>Terratocarcinoma (DA754929, DA758978)<br>Tongue tumor (DA450129) | Lymphoma (BQ049808)<br>Osteosarcoma (BG113716)<br>Neuroepithelioma (DA903910)<br>Lymphoma (CR747151)<br>293T cell line (this study) | AL136881<br>AK290182<br>AM392812 |
| *SECISBP2*_Δ2 | 1–3a,4,5 ... | 2 | ES cell line (CV811081) | | 293T cell line (this study) | |
| *SECISBP2*_Δ3 | 1,2–4,5 ... | 3 | Testis (DB459197) | Genitourinary tract high-grade tumor (AW630547)<br>Mammary gland tumor (BP313796) | | |
| *SECISBP2*_Δ7a | 1–5,6b–7b ... | 3 | Uterus (AI129567, AI128470) | | | AB208940 |
| *SECISBP2*_7c | ... 3,4,5, 6a–7c ... (aa TRAD) | 5 | ES cell line (CN256603, CX787609) | Squamous cell carcinoma (BP352801)<br>Large cell carcinoma (BQ430224) | Ovary terato-carcinoma cell line (BU850141) | |
| *SBP2*_ 7d | ... 3,4,5, 6a–7d ... (aa TRD) | 5 | Pancreas (BU069273)<br>ES cell line (DN602260) | Retinoblastoma (BC001189, BE779955) | Prostate cancer (EC508545) | |
| SECISBP2_Δ9 | ... 8–10 ... | 2 | Retinal pigment epithelium (CA389610) | Leiomyosarcoma (BU902304) | | |

SECISBP2 transcripts that were identified experimentally or by EST database searches are listed according to the nomenclature proposed in the text. Information on exon combination, number of ESTs present, tissue of origin and corresponding GenBank accession numbers are given. ES = embryonic stem.

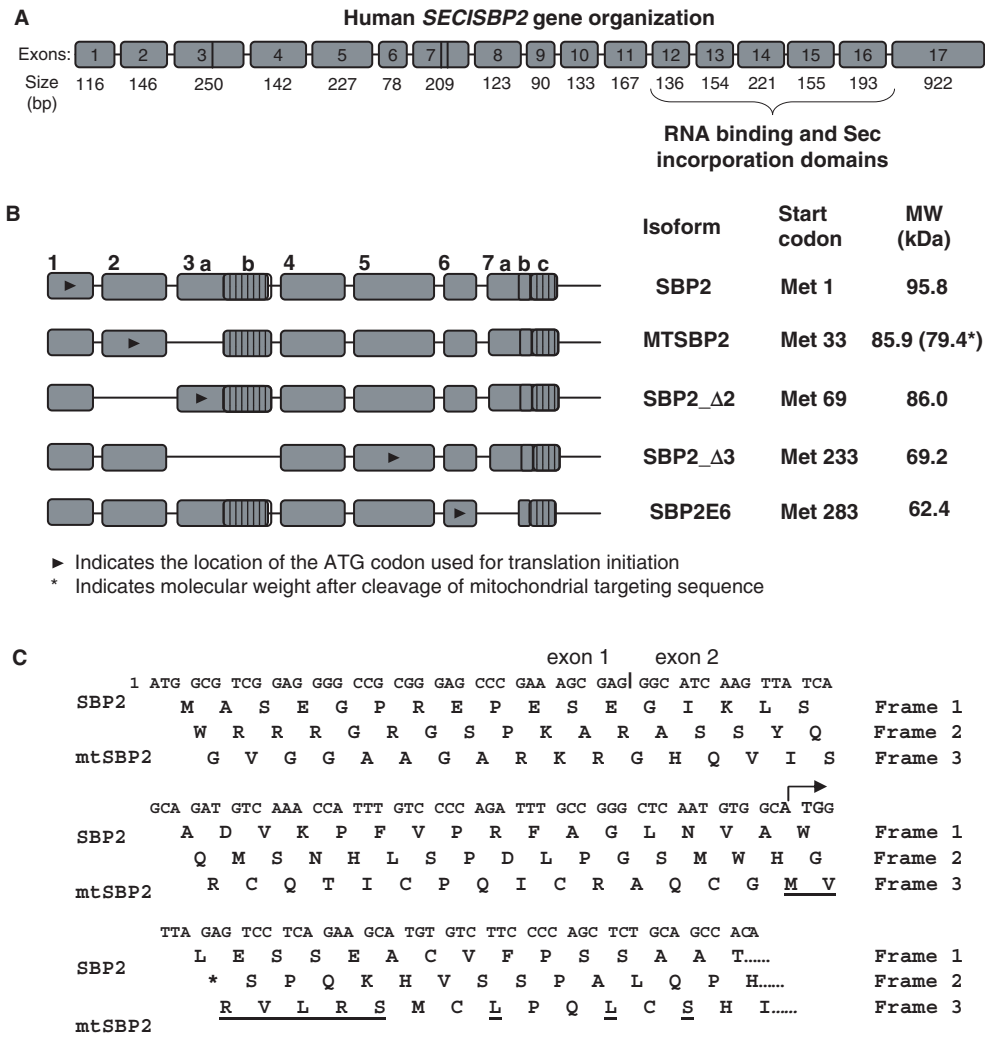


**Figure 1.** Schematic representation of human *SECISBP2* transcript variants. **(A)** Genomic organisation of *SECISBP2* showing the 17 exons and their sizes in base pairs (bp). Locations of the functional domains are indicated. **(B)** Alternatively spliced *SECISBP2* transcript variants generated through different exon combinations are shown schematically. Arrowheads indicate translation start sites. Designation for the encoded protein isoforms, the corresponding Met start codon number [based on numbering in the full-length human SBP2 sequence (NP_076982)] and predicted molecular weights (MW) of isoforms are indicated to the right of each transcript. **(C)** An alternative reading frame used for translation of the mitochondrial SBP2 isoform (mtSBP2) initiates in exon 2 (indicated by arrow). The encoded mitochondrial targeting sequence is underlined.

**Table 2.** Splice site boundaries of *SECISBP2* transcript variants

| Donor exon (nt) | Acceptor exon (nt) | Intro size(kb) | EXON/intron/EXON (splice site consensus: …AG\|gu ragu…$(y)_{10\text{-}15}$nyag\|G…) |
|---|---|---|---|
| 1 (116) | 2 (146) | 1.04 | …AGCG**AG**\|**gu**aagg…*ucauauuuuuccuc*ag\|GGCAUC… |
| 1 (116) | *3a (121) | 6.81 | …AGCG**AG**\|**gu**aagg…*uuuacacuuuuuacuu*ag\|GCAGAA… |
| 2 (146) | *3a (121) | 5.63 | …GACAGA\|**gu**augu…*uuuacacuuuuuacuu*ag\|GCAGAA… |
| 2 (146) | *3b (129) | 5.63 | …GACAGA\|**gu**augu…*uacccuugacuccacac*ag\|AAUGUU… |
| 2 (146) | 4 (142) | 5.63 | …GACAGA\|**gu**augu…*uuuuuaaucuuuccug*cag\|AAGAAA |
| 3 (250) | 4 (142) | 0.20 | …UUUA**AG**\|**gu**gagu…*uuuuuaaucuuuccug*cag\|AAGAAA… |
| 4 (142) | 5 (227) | 2.67 | …AAUC**AG**\|**gu**aaaa…*uuuaauuuuguaauuac*ag\|AUGGUU… |
| 5 (227) | 6 (78) | 4.02 | …UCAA**AG**\|**gu**gagg…*uaauguguuugcuuuuua*g\|GGUGAA… |
| 6 (79) | *7a (209) | 1.53 | …CAAG**AG**\|**gu**aaaa…*uuuuggguuaucuuuga*gc**ag**\|AGUUAU… |
| 6 (79) | *7b (171) | 1.53 | …CAAG**AG**\|**gu**uaucuu…guuauguuguucgac**ag**\|ACAUUA… |
| 6 (79) | *7c (95) | 1.53 | …CAAG**AG**\|**gu**aaaa…*accauuucauc*ag\|CAGAUG… |
| 6 (79) | *7d (92) | 1.53 | …CAAG**AG**\|**gu**aaaa…*ccauugcuucag*cag\|AUCCU… |
| 8 (123) | 10 (132) | 2.76 | …AUUGAA\|**gu**aguac…*uuuugaacuuuc*ag\|GAUAAU… |

The donor and acceptor exons are listed with their sizes in nucleotides (nt) in brackets. Intron sizes are given in kilobases (kb). Boundaries of splice sites was identified from the genomic DNA sequence (http://genome.ucsc.edu) and compared to the consensus of splice site motifs (16). Consensus nucleotides at the 5′ and 3′ splice sites are indicated in bold letters and splice sites are indicated with a vertical line. The polypyrimidine stretch is shown in italics.
*Exons with alternative donor or acceptor sites.

with the eukaryotic Sec-decoding trait. Several alternatively spliced transcripts were found in EST and genomic databases of different organisms, some of which were identical to human *SECISBP2*. Because the mtSBP2 is the most common isoform after full-length SBP2 in humans, we were particularly interested in its evolutionary conservation and existence in other species. Interestingly, sequence comparison between exon 2 of human *SECISBP2* and other homologs revealed that the ATG codon is conserved in chicken, sheep, pig, cow and monkey but not in mouse, rat and dog where it is present as GTG or CTG, which are possible weak translation initiation codons. However, we did not detect ESTs representing *mtSECISBP2* in other organisms except for a distant homolog containing a strong predicted MTS (but low sequence similarity to human MTS) in chicken. It thus appears that the predicted mtSBP2 isoform may be specific to humans.

### Characterization of SBP2 splicing *in vivo* and modulation with antisense oligonucleotides

The identification of alternative splicing within the 5′-region of human *SECISBP2* prompted us to further characterize and quantify the occurrence of these events *in vivo*. We were particularly interested in the *mtSECISBP2* variant since it appeared to be the best represented transcript after the full-length transcript. To gain a better insight into the expression pattern of the two transcripts, we first quantified their relative expression levels in a cDNA panel from various human tissues by real-time RT-PCR using isoform-specific primers spanning the exon 2–3a boundary for *SECISBP2*, and the exon 2–3b boundary for *mtSECISBP2*. As shown in Figure 2A, *SECISBP2* and *mtSECISBP2* were expressed in all tissues tested, with the highest expression levels for both transcripts in testis. The ratio between the *SECISBP2* and *mtSECISBP2* was on average ∼4.4 : 1 in most tissues, which is consistent with the bioinformatics data presented in Table 1. However, colon, thymus and leucocytes had a ∼2 : 1 ratio, indicating that *mtSECISBP2* is most abundantly expressed relative to *SECISBP2* in these tissues. We also confirmed the expression of *mtSECISBP2* variant in a number of normal and cancer-derived cell lines including ones used in this study (data not shown).

As a second approach to characterize and potentially modulate *SECISBP2* splicing *in vivo*, we generated a *SECISBP2* minigene construct (WT minigene), schematically presented in Figure 2B. We also generated two mutant minigene constructs: one harbouring a point mutation at the exon 3a 3′ splice site $^{359}$AG>AA (named Ex3AG>AAΔT) which should abrogate the splicing at this site and hence deplete the production of *mtSECISBP2*; and a second construct harbouring a point mutation ($^{99}$ATG>CTG) to abrogate mtSBP2 start codon in exon 2 (named Ex2ATG>CTG). The minigenes were transfected into C33A cells and products were analyzed by RT-PCR using primers specific to the minigene-derived transcripts as indicated in Figure 2B. The α-$^{32}$P-dCTP labeled products were separated by native PAGE and verified by sequencing. As shown in Figure 2C, lane 1, full-length *SECISBP2* was the predominant transcript expressed from the WT minigene, followed by *mtSECISBP2* and *SECISBP2*_Δ2. These results confirmed that *mtSECISBP2* may indeed be the second most abundant *SECISBP2* transcript. Notably, the Ex3AG>AA mutation indeed abrogated the exon 3a 3′ splice site responsible for the skipping of exon 3a, which is clearly evident by the absence of the mtSBP2 encoding transcript (Figure 2C, lane 2). This observation also conclusively confirmed the existence of an alternative acceptor site within exon 3, and shows that this site is required for production of the *mtSECISBP2* transcript. As expected, the ATG mutant minigene showed no difference in splicing compared to the WT minigene (Figure 2C, lane 3).

ASO with a 2′-*O*-methyl modified ribonucleotide with phosphorothioate backbone have been used to manipulate pre-mRNA splicing in the spinal muscular atrophy gene, *SMN2* (30). This backbone modification imparts a very high affinity for targeted mRNA, resistance to both exo- and endonucleases and does not support cleavage of hybridized mRNA by RNAse H (31). We employed this technology to test whether splicing of the *mtSECISBP2* can be enhanced using a 23-mer ASO complementary to the last 19 nt of intron 2 and the first four nucleotides of exon 3a (named In2E3a). This was expected to promote exon 3a skipping and thus block splicing of the full-length transcript and enhance the production of the mtSBP2-encoding transcript. An unrelated ASO was used as control. Resulting PCR products from cells co-transfected with the In2E3a, or control ASO, and the WT minigene are shown in Figure 2C, lanes 4 and 5. Notably, the In2E3a ASO efficiently blocked splicing at the exon 3a site, thus, promoting exon 3a skipping as shown by a dramatic reduction in full-length transcript levels and a corresponding increase in *mtSECISBP2* transcript (lane 4), while the control ASO had no effect on the splicing pattern (lane 5 compared to lane 1). Similar results were obtained in HeLa cells (data not shown). The In2E3a ASO was also efficient in altering the splicing of the endogenous *SECISBP2* transcript in several cell lines, as measured by real-time RT-PCR with isoform-specific primers. Generally, a 2- to 4-fold increase in exon 3a skipping with a corresponding 50–60% decrease in exon 3a inclusion was obtained in cell lines including C33A, HeLa and untransformed human fibroblast cells (NFF). Results from NFF cells are shown in figure 2D. Taken together, these findings demonstrated that the In2E3a ASO can be used as an efficient tool to promote SBP2 exon 3a skipping *in vivo*, and to generate predominantly the mtSBP2-encoding transcript from *SECISBP2* gene.

### Several SBP2 isoforms are expressed from the minigene

We next investigated the translation pattern of the alternatively spliced SBP2 isoforms using the minigene constructs. These were transiently transfected in several cell lines including 293T, C33A and HeLa, and the expressed proteins were analyzed by western blotting. Blots were probed with anti-GFP antibodies (which is tagged at the C-terminus of SBP2), and with anti-SBP2 antibodies raised against a central region of SBP2 (exon 6–8) to

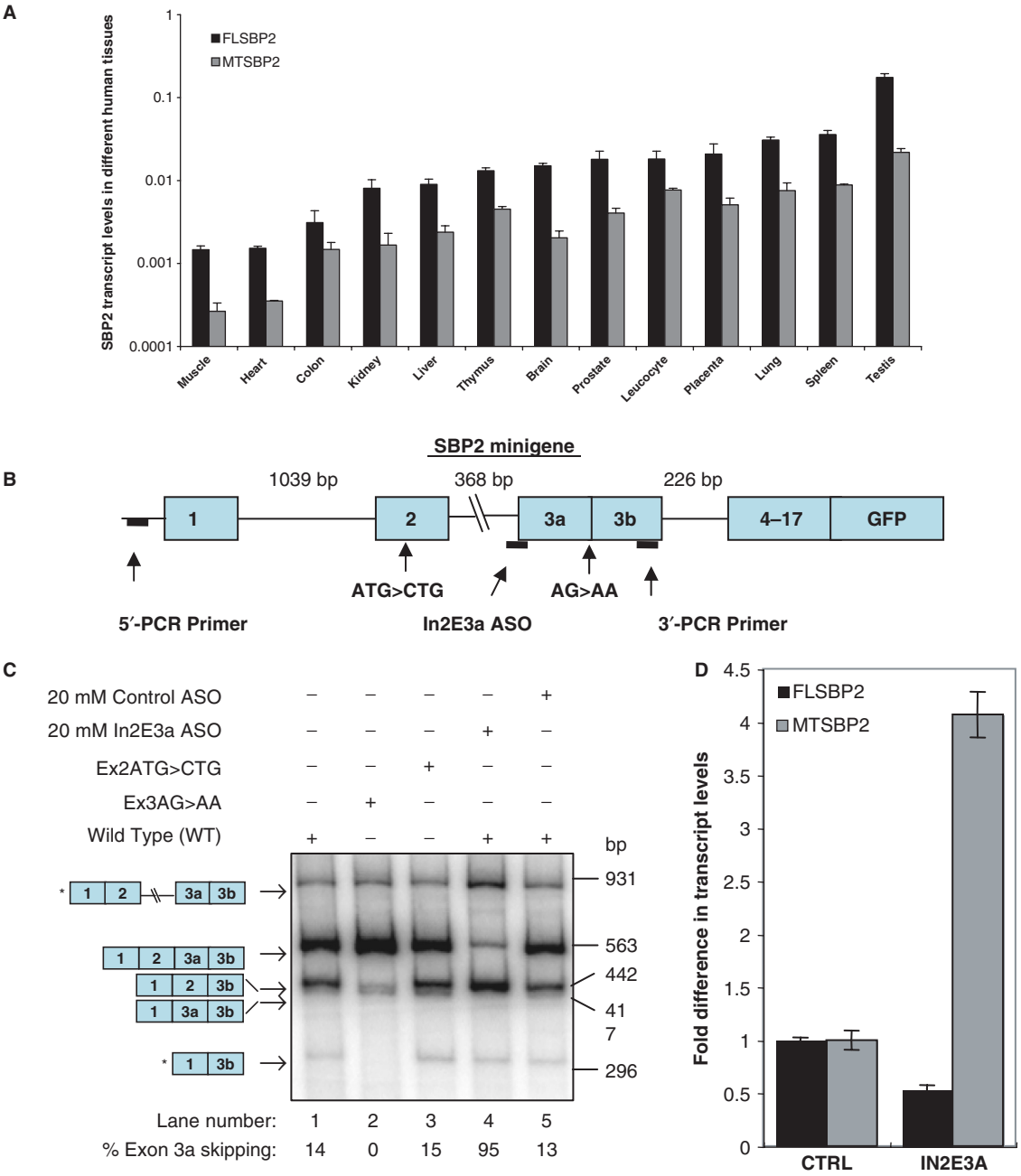


**Figure 2.** *SECISBP2* transcript expression and minigene-based *in vivo* splicing assay. **(A)** Relative expression levels of full-length and mitochondrial SBP2 transcripts in a cDNA panel of human tissues was analyzed by real-time PCR using transcript specific primers. Data was analyzed using the deltaCT method. **(B)** Schematic representation of the *SECISBP2* minigene indicating exon/intron composition, location of primers used to amplify the minigene-expressed products, annealing site for antisense oligonucleotides (In2E3a ASO) and location of mutations introduced. **(C)** *In vivo* splicing pattern of *SECISBP2* minigene constructs. RT-PCR of $\alpha$-$^{32}$P-dCTP labeled products were amplified from C33A cells transfected with wild-type (WT), exon 2 ATG>CTG mutant (Ex2ATG>CTG) and exon 3 AG>AA mutant (Ex3AG>AA) minigenes. The exon combination as verified by sequencing is indicated on the left (products indicated by $*$ are predicted only). Mutation at the exon 3a acceptor site AG>AA abolishes splicing between exon 2 and exon 3b as shown by the absence of exon 2–3b spliced product (lane 2). In2E3a ASO treatment almost completely abrogates exon 2–3a splicing and thus full-length *SECISBP2* transcript and dramatically increases exon 2–3b splicing and *mtSECISBP2* transcript levels (lane 4). Percentage of exon 3a skipping was calculated from the total value of exon 3a-included and exon 3a-skipped products. **(D)** Normal human fibroblast cells were treated with In2E3a ASO and levels of *SECISBP2* and *mtSECISBP2* were measured by real-time RT-PCR. In2E3a-treated cells show a 4-fold increase in *mtSECISBP2* and 50% decrease in the full-length *SECISBP2* transcript.

ensure that the proteins detected are products that initiate at different ATG codons within the N-terminal region of SBP2 rather than degradation products. A representative example of the minigenes' expression pattern in 293T cells is shown Figure 3A. Consistent with the data obtained from the splicing assay, full-length SBP2 initiating from the ATG in exon 1, was by far the highest expressed protein from the WT and Ex2ATG>CTG minigenes

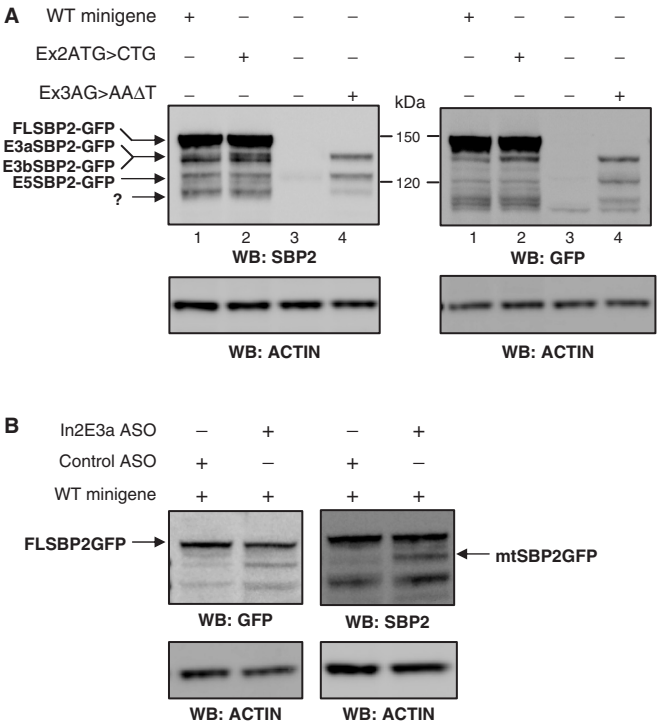


**Figure 3.** Minigene-based expression of SBP2 isoforms. **(A)** The minigenes (described in the legend to Figure 2) were transfected into 293T cells and the proteins expressed were separated on 4–12% gradient gels and analyzed by western blotting with anti-GFP and anti-SBP2 antibodies. Western blots with the two antibodies show similar staining pattern and thus confirm the expression of several SBP2 isoforms initiating from alternative ATG codons. E3aSBP2-GFP, E3bSBP2-GFP and E5SBP2-GFP refer to isoforms initiating at ATG codons in exons 3a, 3b and 5 respectively. **(B)** Western blots of cells co-transfected with wild-type (WT) minigene and the In2E3a antisense oligonucleotides that promotes splicing of the *mtSECISBP2* transcript show translation of the mtSBP2GFP isoform. Actin was used as a control for protein loading.

(Figure 3A lanes 1 and 2), however, the presence of multiple bands detected by both antibodies suggested that proteins initiating from other ATG start codons are expressed. Due to the small differences in their size (85.9 kDa, 86 kDa, 80 kDa) some of them could not be resolved and identified easily. However, the nucleotide deletion ($T^{367}$) in exon 3b of the Ex3AG >AAΔT minigene which abrogates the ORFs starting at ATG codons in exons 1, 2 or 3a by creating PTCs, enabled us to identify two of the additional bands as the SBP2 isoforms initiating in exon 3b from Met 139 and in exon 5 from Met 233 (Figure 3A lane 4). Thus, using the minigene-based *in vivo* splicing assay we have been able to convincingly show that alternative splicing of *SECISBP2* may have a functional relevance as multiple SBP2 isoforms initiating from different ATG start codons and containing different N-termini amino acid composition are being expressed.

Intriguingly, we could not detect a decrease in a band representing the mtSBP2 protein expressed from the Ex2ATG>CTG mutant construct (Figure 3A lane 2). On the contrary, a small increase in expression of the band below the full-length SBP2 was consistently seen (Figure 3A lane 2). According to molecular weight prediction, this band could represent a protein initiating from ATG codons in exon 3a or exon 3b. We speculate that the increased expression of this band in the Ex2ATG>CTG mutant could be the consequence of lack of translation initiation in exon 2 due to abrogation of the ATG codon with a consequent promotion of translation from downstream ATG codons. Although we could not detect the mtSBP2 isoform expressed from the minigene by western blotting, its expression levels could be below the detection limit, but still responsible for regulating the expression of other downstream ATG-initiating isoforms (Figure 3A lane 1 compared to lane 2). However, this possibility remains to be investigated. We also noted that translation of the SBP2E3b isoform from the Ex3AG>AAΔT minigene did not increase significantly when a point mutation that abrogates the full-length SBP2 reading frame is introduced (Figure 3A lane 4). This suggests that the ATG codon context in exon 3b is rather weak, or that expression of this isoform is strictly regulated. The overall SBP2 splicing pattern was similar in other cell lines tested despite variations in transfection efficiency (data not shown).

We showed above (Figure 2B) that the In2E3a ASO is extremely efficient at increasing the levels of the *mtSECISBP2* transcript both off the minigene and endogenously. We therefore tested if co-transfecting the WT minigene with the In2E3A ASO could induce the expression of the mtSBP2 protein. As shown Figure 3B, a band that corresponds to the predicted size of mtSBP2-GFP was indeed apparent in In2E3a ASO co-transfected cells, but not in control ASO transfected cells, demonstrating that this isoform can be translated *in vivo*, albeit very inefficiently. Although the In2E3a ASO proved efficient at inducing splicing of endogenous *mtSECISBP2* transcript, we were unable to detect the endogenous mtSBP2 protein following In2E3a ASO transfection, despite extensive attempts in several cell lines. Overall, these results showed that full-length *SECISBP2* is the most abundant and preferentially translated SBP2-encoding transcript. However, the alternatively spliced transcripts generated are also translated into protein, albeit far less efficiently.

### The mtSBP2 isoform localizes to mitochondria

One of the main aims of the minigene splicing assay was to analyze the expression and localization of the protein encoded by the most common alternate *SECISBP2* transcript-mtSBP2. Although the assay convincingly showed expression of the *mtSECISBP2* transcript, it proved less amenable at analyzing the protein expression. Thus, in order to determine if the predicted mtSBP2 does indeed localize to mitochondria, we expressed the mtSBP2-encoding cDNA (commencing at the ATG codon in exon 2) fused N-terminal to GFP (mtSBP2-GFP) in C33A cells, and analyzed its subcellular localization by co-staining with the mitochondrial marker MitoTracker Red CMX-Ros. The full-length FLSBP2-GFP construct and a construct lacking the putative MTS encoded by the alternate reading frame in exon 2 (SBP2_Δ2-GFP) were used for comparison. Localization of the proteins was visualized using a Z-scanning

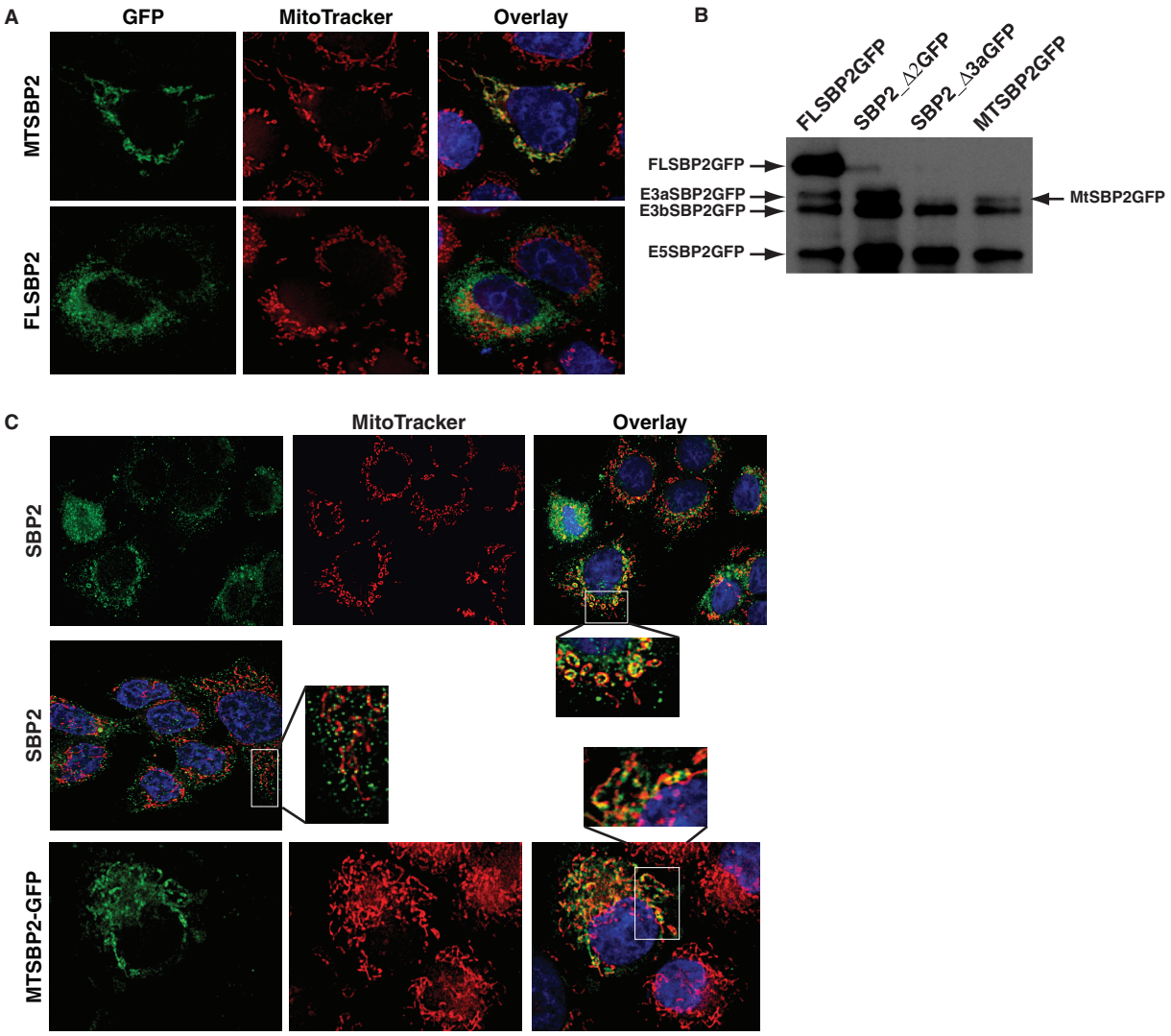


**Figure 4.** Localization of over-expressed mtSBP2-GFP and endogenous mtSBP2 isoform at the mitochondria. **(A)** The localization of GFP-tagged full-length (FLSBP2-GFP) and mitochondrial SBP2 isoforms (mtSBP2-GFP) in C33A cells was visualized by fluorescence microscopy. Mitochondria were stained with MitoTracker Red CMX-Ros. Single Z-layer deconvolution images show strong mitochondrial localization of mtSBP2-GFP (yellow) but not of FLSBP2-GFP. **(B)** Western blot of SBP2 isoforms expressed from cDNAs as GFP-fusion proteins. SBP2_Δ2-GFP and SBP2_Δ3a-GFP lack exons 2 and 3a respectively. mtSBP2-GFP cDNA begins at the ATG in exon 2. These proteins were resolved on a 6% SDS–PAGE gel, which yielded a higher level of separation compared to Figure 3. **(C)** High resolution single Z-layer deconvolution images show the localization of mtSBP2-GFP and endogenous mtSBP2 proteins at the mitochondria in C33A cells. 10% of cells display strong mitochondrial staining as shown by the yellow staining in the top panel enlargement, while in most cells only a few dots were detected within the mitochondria (middle panel). Immunofluorescence staining was performed with the anti-SBP2 antibody EC1. Enlargements show a similar punctated staining pattern along the mitochondria for both mtSBP2-GFP (bottom panel) and endogenous mtSBP2.

microscope followed by image deconvolution. Interestingly, mtSBP2-GFP expressing cells exhibited distinct cytoplasmic fluorescence, which overlapped significantly with the MitoTracker staining as indicated by the intense yellow staining in Figure 4A (Pearson coefficient 0.879). FLSBP2-GFP protein displayed a strong peri-nuclear punctate staining, however, this fluorescence did not overlap significantly with the MitoTracker staining (Figure 4A bottom panels, Pearson coefficient 0.264). Most likely, this pattern represents a ribosomal/endoplasmic reticulum (ER) staining which is the believed functional localization of SBP2 (14,32). Similar to FLSBP2-GFP, SBP2_Δ2-GFP localized throughout the cytoplasm and showed marginal co-localization with MitoTracker (data not shown). This data established that the MTS encoded by the alternative reading frame in exon 2 is functional, and required for targeting the mtSBP2-GFP protein to the mitochondria. It should be noted that only ~10% of cells transfected with the mtSBP2-GFP plasmid displayed strong mitochondrial localization as shown in Figure 4A, and some of the transfected cells also displayed a diffuse cytoplasmic fluorescence that did not co-localize with the MitoTracker staining (data not shown). Indeed, western blot of mtSBP2-GFP transfected cells showed the presence of additional proteins initiating in exon 3b and exon 5 (Figure 4B, lane 4), which explained the cytoplasmic

fluorescence observed. Notably, mtSBP2-GFP was poorly expressed in comparison to other isoforms and we consistently observed this in several cell lines tested. It is also interesting to note that cells transfected with a construct that lacks exon 2 (SBP2_Δ2-GFP) expressed high levels of proteins initiating in exons 3a, 3b and 5 (Figure 4B, lane 4), while lack of exon 3a (SBP2_Δ3a-GFP) did not seem to have a similar effect on proteins initiating in exons 3b and 5 (Figure 4B, lane 3). These results suggest that exon 2 might play a role in regulating the expression of some of the SBP2 isoforms by suppressing translation initiation at ATG start sites in exons 3a, 3b and 5. These results are also in agreement with the results from the minigene assay where mutation to the exon 2 ATG start site led to increased translation from exon 3b.

We also sought to determine whether the mtSBP2 isoform, or additional spliced variants could be detected endogenously in cells using our previously described anti-SBP2 antibody raised against an epitope in exons 6–8 (aa 279–378 in SBP2) (14) which should detect most isoforms, if expressed. However, we were unable to detect any SBP2 isoforms other than the full-length SBP2 by western blotting. Similarly, analysis of mitochondrial fractions of cells failed to reveal the existence of mtSBP2 by western blotting and this antibody was not suitable for immunofluorescence-based detection of mtSBP2 due to similar level of staining in SBP2-depleted and normal cells. Notably, a new anti-peptide antibody raised against the C-terminus of SBP2 (referred to as anti-SBP2 EC1) was shown to be very specific for SBP2 (data not shown). We used this antibody in immunofluorescence of C33A cells and found that the majority of cells showed a distinct punctated cytoplasmic staining (Figure 4C, middle panel). Interestingly, while most cells also showed some punctated staining along the mitochodria, ~5–10% of cells displayed a clear mitochondrial SBP2 staining that co-localized strongly with MitoTracker in (Figure 4C, top panel and enlargement). This staining pattern was similar to that observed for overexpressed mtSBP2-GFP (Figure 4C, bottom panel and enlargement). Collectively, these results provide evidence that mtSBP2 contains a functional MTS that targets the mtSBP2-GFP protein to the mitochondria, and also that endogenous mtSBP2 localizes to the mitochondria. Although the EC1 antibody did detect full-length SBP2 by western blotting, we were unable to confirm the presence of mtSBP2 isoform in mitochondrial fractions of cells by this method.

### Coordinated transcriptional and translational regulation of SBP2 following UVA treatment

We previously showed that SBP2 is regulated through redox-state and localization changes, and that these affect selenoprotein synthesis (14). In this study, we wished to investigate if oxidative stress may cause transcriptional changes in *SECISBP2* expression, particularly in the full-length and mitochondrial transcripts. To complement our previous data, we used UVA irradiation, a physiologically relevant oxidative stress inducer that causes intracellular damage by production of oxygen singlet ($O_2^{\bullet -}$) molecules. To monitor the transcriptional response of SBP2, HeLa cells were exposed to 50 kJ/m$^2$ UVA irradiation and allowed to recover for the indicated amounts of time, and *SECISBP2* and *mtSECISBP2* transcript levels were measured by real-time RT-PCR. Interestingly, we found that both transcripts were induced by almost 3-fold immediately after UVA treatment, followed by a sharp decline at 2 h and subsequent stabilization of both transcripts for up to 24 h (Figure 5A). Importantly, these results show that both transcripts are regulated in a similar manner in response to oxidative stress. The response to UVA treatment at the protein level correlates well with the transcriptional response. We observed a rapid degradation of SBP2 with levels down to ~30% of mock-treated cells at 0 h after treatment (Figure 5B). Interestingly and as reported previously (33), the stress sensor HSP70 protein was stabilized in response to UVA treatment and remained elevated for 16 h post treatment (Figure 5B). We believe that the rapid degradation of SBP2 during the course of UVA irradiation is the trigger for the concomitant transcriptional induction seen in Figure 5A. Although, SBP2 protein levels recovered slightly at 2 h post treatment, they remained at only ~50% of the initial levels for up to 8 h and returned to the initial starting levels by 24 h post treatment. These results are consistent with our previous observations that selenoprotein synthesis is inhibited in response to oxidative stress and suggest that down regulation of SBP2 protein levels might provide additional mechanistic explanation for those observations (6,14).

We also investigated the UVA stress response pattern of the SBP2 isoforms expressed by the minigene constructs. We conducted a similar time course experiment in response to UVA treatment in HeLa cells expressing wild-type SBP2 protein (WT-SBP2GFP), the exon 2 ATG>CTG mutated SBP2 (ATGm-SBP2GFP) and the SBP2 mutated protein that initiates translation from exon 3b (E3b-SBP2GFP). As shown in Figure 5C, all minigene products showed a similar down-regulation pattern in response to stress, as seen for endogenous SBP2. Similar results were obtained in NFF cells (data not shown). From these experiments we thus conclude that mutation of the ATG codon in exon 2 and thus the lack of mtSBP2 expression does not affect the response of the full-length SBP2 to UVA-induced oxidative stress, and that the spliced variants E3b-SBP2GFP and E5-SBP2GFP (data not shown) have a similar pattern of regulation as full-length SBP2 in response to stress. Importantly, these experiments established a coordinated transcriptional and translational mechanism of SBP2 regulation in response to oxidative stress, and revealed that the alternatively spliced transcripts and the corresponding proteins have a similar pattern of regulation as the full-length SBP2.

## DISCUSSION

SBP2 is a critical factor for selenoprotein synthesis, with roles in SECIS element binding, ribosome binding and Sec incorporation. Much of recent work has elaborated on

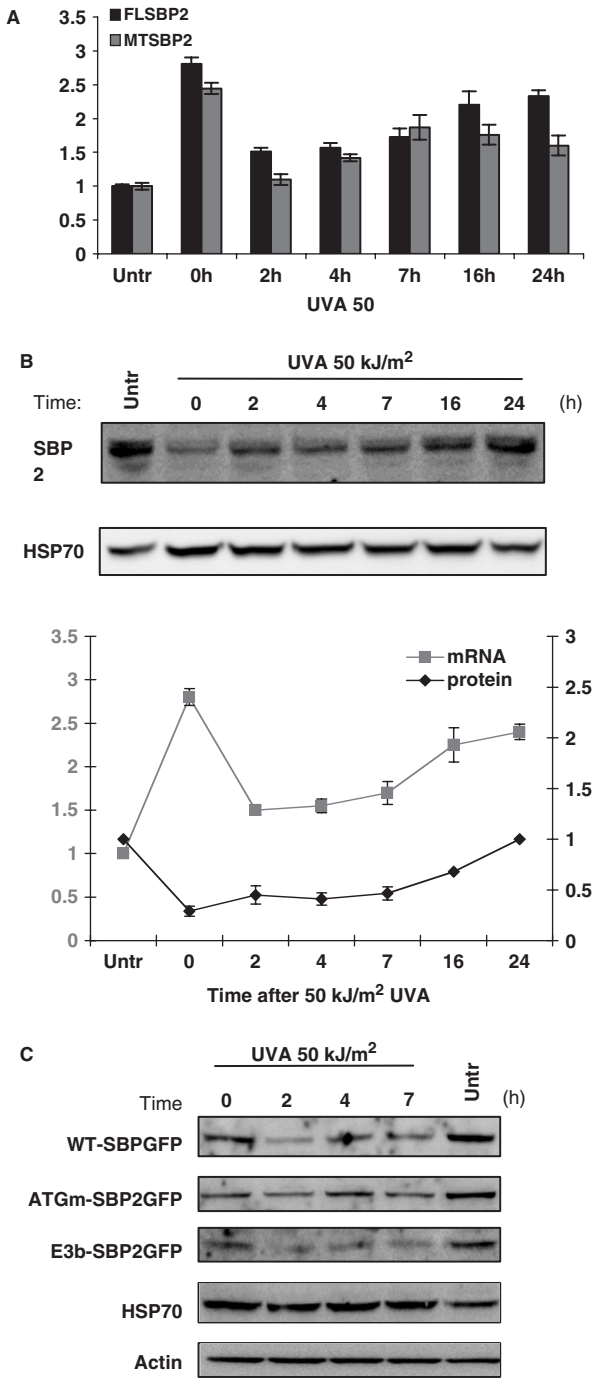


**Figure 5.** Coordinated transcriptional and translational regulation of SBP2 following UVA treatment. Transcriptional and translational response of full-length SBP2 (FLBSP2) and mitochondrial SBP2 (mtSBP2) following 50 kJ/m$^2$ of UVA irradiation was monitored in HeLa cells over 24 h. **(A)** Real-time RT-PCR using transcript specific primers shows a similar transcriptional induction of both transcripts in response to treatment. **(B)** Western blot using anti-SBP2 antibodies shows the translational response of endogenous SBP2 and HSP70 at different time points after UVA irradiation. Quantitation of FLSBP2 transcript and protein levels is presented in the graph below. Error bars represent the standard error of the mean (SEM). Transcript levels were normalized against GAPDH and protein levels were normalized against actin. **(C)** Western blots show the translational response of WT, Ex2ATG>CTG and Ex3AG>AA minigene-derived proteins to UVA treatment. HSP70 was used as a marker for UVA-induced stress and actin shows protein loading.

understanding its role in the translation of 25 mammalian selenoproteins, by detailed molecular and biochemical characterization. Mutations in the *SECISBP2* gene that either alter the reading frame through splicing defects or alter the interaction of SBP2 with a subset of SECIS elements due to amino acid substitutions, result in abnormal thyroid hormone function in humans (15,25). In this study, we presented the first detailed *in vivo* and *in silico* characterization of human *SECISBP2* alternative splicing and highlighted a new mode of transcriptional and translational regulation. Interestingly and intriguingly, the most abundant SBP2 variant after the full-length SBP2 contains a MTS, which we showed is functional and required for targeting of the mtSBP2 protein to mitochondria. A small proportion of the endogenous SBP2 pool is also localized to the mitochondria, however, only a small fraction of cells appeared to have strong mitochondrial SBP2 localization. This suggests that the mitochondrial localization of SBP2 may be tightly regulated and may occur predominantly during certain, yet unidentified conditions.

The identification of a potential mitochondrial human-specific SBP2 isoform was an intriguing and somewhat puzzling finding when viewed against the known SBP2 function in decoding UGA as Sec during selenoprotein translation. This process is unlikely to occur within the inner mitochondria for the following reasons: (i) analysis of the mitochondrial genome using the SECISearch program (34) suggests that the human mitochondrial genome does not contain any genes with SECIS elements and hence does not encode selenoproteins; (ii) UGA codes for tryptophan in the human mitochondrial genome; and (iii) mitochondrial matrix translation uses a mechanism similar to that of prokaryotes. These facts would argue against the requirement of a mitochondrial SBP2 isoform with canonical function in Sec incorporation. However, emerging evidence suggests that translationally active cytoplasmic ribosomes, or polysomes, are present on the outer membrane of the mitochondria and that about 50% of mRNAs coding for mitochondria-localized products are primarily associated with mitochondria-bound polysomes (35–37). Targeting mRNAs to the mitochondria is mediated by conserved secondary structures in their 3′ UTR (36). Although this process is poorly understood, it is possible that the conservation of localized translation might assist in the co-translational import of hydrophobic proteins into mitochondria to prevent their aggregation in the cytoplasm, or to simply provide a more efficient way of translation, as one mRNA molecule can serve in several rounds of translation. The mitochondrial SBP2 isoform could thus function in the translation of selenoproteins targeted to mitochondria such as thioredoxin reductase 2 (TxnRd2/TR3) (1,38), mitochondrial form of phospholipid glutathione peroxidase (PHGPx/GPx4) (39) and glutathione peroxidase 1 (GPx1) (40) on mitochondria-bound cytoplasmic ribosomes. Alternatively, mtSBP2 could be involved in binding to mRNA structures, possibly also in non-selenoprotein encoding mRNAs that target the message to the outer mitochondrial ribosomes. The high-resolution images we obtained of both over-expressed mtSBP2-GFP and endogenous mtSBP2 pointed

to a localization of the mtSBP2 isoform on the outer mitochondrial surface, in specific punctate clusters. This localization would indeed be in agreement with the functional localization of SBP2 at polysomes. The fact that we could not detect mtSBP2 in mitochondrial subfractions of cells by western blotting argues for a possible loose interaction between mtSBP2 and the organelle, which may be easily disrupted during the fractionation procedure. But if mtSBP2 is localized on the outer surface of the mitochondria, why would it require a classical type of MTS that generally targets proteins to the inner mitochondrial matrix? Although this question remains to be answered, our findings are relevant to a recent report showing that DAKAP1, a multifunctional protein with roles in cAMP dependent protein kinase (PKA) regulation and mRNA binding, can be targeted to the cytosolic side of the outer membrane of the mitochondria by use of a classical MTS. DAKAP1 contains a bi-functional targeting motif that switches to encode either an MTS, such as the one present in mtSBP2, or an ER targeting signal (41). Although the precise mechanism of how this protein attaches to the mitochondria outer membrane remains unknown at present, it is possible to reconcile the idea that proteins that localize on the cytosolic side of the mitochondrial membrane can be targeted there by classical MTSs. The MTS in mtSBP2 may thus facilitate the localization of the protein to the cytosolic side of the mitochondria via active mitochondrial import. More detailed studies will be required to investigate this aspect of mtSBP2 localization as well as the precise role of this isoform in the cell. The low expression of mtSBP2 isoform in the cell lines tested indicates that its synthesis could be dependent on tissue-specific translation factors and may be maximized in tissues or organs with high demand for mitochondrial selenoproteins. A prime candidate would be testis, where PHGPx is the most abundant selenoprotein. Indeed, the expression of both full-length *SECISBP2* and *mtSECISBP2* transcripts was highest in testis when compared to twelve other tissues, providing additional proof to strengthen this hypothesis.

This study established that human *SECISBP2* has an extensive alternative splicing pattern in the 5′-region. Some of the splicing events provoke ORF alterations, which lead to premature termination codons, thus promoting translation from downstream ATG start codons. Our *in vivo* splicing assay and treatment with ASOs showed that at least four additional ATG start codons in exons 2, 3a, 3b and 5 are used to produce proteins with different N-terminal amino acid sequence such as mtSBP2, or N-terminally truncated SBP2 isoforms. Because all alternative splicing events within SBP2 are confined within the region dispensable for Sec incorporation *in vitro*, it is reasonable to postulate that these events are unlikely to affect RNA binding *per se*, however, this level of regulation may play a fine-tuning or regulatory role in SBP2-dependent Sec incorporation function *in vivo*. The role of the N-terminal region of SBP2 is a puzzling, yet unanswered, question in the field. So far, the only characterized motif within this region is a nuclear localization signal (NLS) that enables SBP2 to shuttle between the nucleus and cytoplasm (14), however, its requirement for selenoprotein synthesis *in vivo* has not been determined. Interestingly, the NLS is located within exon 8, which is common to all alternatively spliced SBP2 isoforms suggesting that this motif may indeed play an important role in the function of SBP2 in the nucleus *in vivo*. Consistent with this, recent studies have suggested a new role of SBP2 in protection of selenoprotein encoding mRNAs from nonsense mediated decay by binding to these mRNAs in the nucleus (42,43).

The human selenoproteome consists of 25 selenoproteins (44) but the SECIS core element and the binding site for SBP2 are well conserved. As a result, Sec incorporation with regard to SECIS element binding would not require variability within the SBP2 RNA binding region which could explain the lack of alternate splicing in the C-terminal region of SBP2. In contrast, the hierarchy of selenoprotein synthesis is expected to involve specific factors that may dictate the differential binding of SBP2 to different selenoprotein mRNAs (25,43). The high sequence variability in the N-terminal region of SBP2 could thus serve as a protein–protein interaction domain and function in the recruitment of such factors prior to interaction with the SECIS element.

In a previous study we showed that acute oxidative stress caused by $H_2O_2$ and sodium selenite had an inhibitory effect on selenoprotein synthesis, and that this was mediated by oxidation of SBP2 redox-sensitive cysteine residues and its depletion from the ribosomes (14). In the current study, using UVA-irradiation as a cause of oxidative stress we found that SBP2 responded by coordinated transcriptional and translational changes following stress. Importantly, *SECISBP2* and *mtSECISBP2* transcripts were simultaneously and immediately induced during treatment, and stabilized during the recovery phase. At the protein level, SBP2 was degraded and levels remained approximately half of the initial levels for ~16 h post-irradiation. The SBP2 isoforms that we could monitor using the minigene showed similar down-regulation as full-length SBP2, suggesting that their intracellular function is most likely related to the function of full-length SBP2 in SECIS binding and Sec incorporation. However, our data does not exclude the possibility that mtSBP2 or any other SBP2 isoforms may perform additional functions unrelated to selenium metabolism.

This is the first report validating the occurrence and significance of alternative splicing associated with *SECISBP2*, an essential gene linked to selenium metabolism. Although, we have focussed mainly on one spliced variant, *mtSECISBP2*, there remain other variants of significant interest. Having shown that an ASO-based approach could be used to generate specific spliced variants, future studies could be tailored to examine their functions. Recent years have seen a dramatic evolution in our understating of translational regulation by microRNAs, a class of small RNA that could be synthesized by a stem-loop containing transcript generated from RNA Polymerase II (45). To a broader significance, it remains to be seen if some of the poorly translatable *SECISBP2* spliced variants including mtSBP2 are meant

to generate microRNAs and/or serve as potential targets of microRNAs.

## SUPPLEMENTARY DATA

Supplementary Data are available at NAR Online.

## ACKNOWLEDGEMENTS

We thank Dr Anna-Klara Rundlof for help with database searches and analyses, Dr Nathan Subramaniam for kindly providing the human cDNA panel and Drs. Armando van der Horst and Derek Richard for critical reading of the manuscript.

## FUNDING

The National Health and Medical Research Council of Australia (to KK.K.); United States National Institutes of Health grants (R01NS055925 and R21NS055149 to R.N.S). Funding for open access charge: Waived by Oxford University Press.

*Conflict of interest statement*. None declared.

## REFERENCES

1. Lee,B.J., Worland,P.J., Davis,J.N., Stadtman,T.C. and Hatfield,D.L. (1989) Identification of a selenocysteyl-tRNA(Ser) in mammalian cells that recognizes the nonsense codon, UGA. *J. Biol. Chem.*, **264**, 9724–9727.
2. Berry,M.J., Banu,L., Chen,Y.Y., Mandel,S.J., Kieffer,J.D., Harney,J.W. and Larsen,P.R. (1991) Recognition of UGA as a selenocysteine codon in type I deiodinase requires sequences in the 3′ untranslated region. *Nature*, **353**, 273–276.
3. Berry,M.J., Banu,L., Harney,J.W. and Larsen,P.R. (1993) Functional characterization of the eukaryotic SECIS elements which direct selenocysteine insertion at UGA codons. *Embo J.*, **12**, 3315–3322.
4. Howard,M.T., Aggarwal,G., Anderson,C.B., Khatri,S., Flanigan,K.M. and Atkins,J.F. (2005) Recoding elements located adjacent to a subset of eukaryal selenocysteine-specifying UGA codons. *Embo J.*, **24**, 1596–1607.
5. Howard,M.T., Moyle,M.W., Aggarwal,G., Carlson,B.A. and Anderson,C.B. (2007) A recoding element that stimulates decoding of UGA codons by Sec tRNA[Ser]Sec. *RNA*, **13**, 912–920.
6. Papp,L.V., Lu,J., Holmgren,A. and Khanna,K.K. (2007) From selenium to selenoproteins: synthesis, identity, and their role in human health. *Antioxid. Redox Signal.*, **9**, 775–806.
7. Copeland,P.R. and Driscoll,D.M. (1999) Purification, redox sensitivity, and RNA binding properties of SECIS-binding protein 2, a protein involved in selenoprotein biosynthesis. *J. Biol. Chem.*, **274**, 25447–25454.
8. Copeland,P.R., Fletcher,J.E., Carlson,B.A., Hatfield,D.L. and Driscoll,D.M. (2000) A novel RNA binding protein, SBP2, is required for the translation of mammalian selenoprotein mRNAs. *Embo J.*, **19**, 306–314.
9. Fagegaltier,D., Hubert,N., Yamada,K., Mizutani,T., Carbon,P. and Krol,A. (2000) Characterization of mSelB, a novel mammalian elongation factor for selenoprotein translation. *Embo J.*, **19**, 4796–4805.
10. Tujebajeva,R.M., Copeland,P.R., Xu,X.M., Carlson,B.A., Harney,J.W., Driscoll,D.M., Hatfield,D.L. and Berry,M.J. (2000) Decoding apparatus for eukaryotic selenocysteine insertion. *EMBO Rep.*, **1**, 158–163.
11. Chavatte,L., Brown,B.A. and Driscoll,D.M. (2005) Ribosomal protein L30 is a component of the UGA-selenocysteine recoding machinery in eukaryotes. *Nat. Struct. Mol. Biol.*, **12**, 408–416.
12. Xu,X.M., Carlson,B.A., Mix,H., Zhang,Y., Saira,K., Glass,R.S., Berry,M.J., Gladyshev,V.N. and Hatfield,D.L. (2007) Biosynthesis of selenocysteine on its tRNA in eukaryotes. *PLoS Biol.*, **5**, e4.
13. Copeland,P.R., Stepanik,V.A. and Driscoll,D.M. (2001) Insight into mammalian selenocysteine insertion: domain structure and ribosome binding properties of Sec insertion sequence binding protein 2. *Mol. Cell. Biol.*, **21**, 1491–1498.
14. Papp,L.V., Lu,J., Striebel,F., Kennedy,D., Holmgren,A. and Khanna,K.K. (2006) The redox state of SECIS binding protein 2 controls its localization and selenocysteine incorporation function. *Mol. Cell. Biol.*, **26**, 4895–4910.
15. Dumitrescu,A.M., Liao,X.H., Abdullah,M.S., Lado-Abeal,J., Majed,F.A., Moeller,L.C., Boran,G., Schomburg,L., Weiss,R.E. and Refetoff,S. (2005) Mutations in SECISBP2 result in abnormal thyroid hormone metabolism. *Nat. Genet.*, **37**, 1247–1252.
16. Matlin,A.J., Clark,F. and Smith,C.W. (2005) Understanding alternative splicing: towards a cellular code. *Nat. Rev. Mol. Cell. Biol.*, **6**, 386–398.
17. Clark,F. and Thanaraj,T.A. (2002) Categorization and characterization of transcript-confirmed constitutively and alternatively spliced introns and exons from human. *Hum. Mol. Genet.*, **11**, 451–464.
18. Lewis,B.P., Green,R.E. and Brenner,S.E. (2003) Evidence for the widespread coupling of alternative splicing and nonsense-mediated mRNA decay in humans. *Proc. Natl Acad. Sci. USA*, **100**, 189–192.
19. Faustino,N.A. and Cooper,T.A. (2003) Pre-mRNA splicing and human disease. *Genes. Dev.*, **17**, 419–437.
20. Wikstrand,C.J., Hale,L.P., Batra,S.K., Hill,M.L., Humphrey,P.A., Kurpad,S.N., McLendon,R.E., Moscatello,D., Pegram,C.N., Reist,C.J. *et al.* (1995) Monoclonal antibodies against EGFRvIII are tumor specific and react with breast and lung carcinomas and malignant gliomas. *Cancer Res.*, **55**, 3140–3148.
21. Naor,D., Nedvetzki,S., Golan,I., Melnik,L. and Faitelson,Y. (2002) CD44 in cancer. *Crit. Rev. Clin. Lab. Sci.*, **39**, 527–579.
22. Saito,H., Nakatsuru,S., Inazawa,J., Nishihira,T., Park,J.G. and Nakamura,Y. (1997) Frequent association of alternative splicing of NER, a nuclear hormone receptor gene in cancer tissues. *Oncogene*, **14**, 617–621.
23. Orban,T.I. and Olah,E. (2003) Emerging roles of BRCA1 alternative splicing. *Mol. Pathol.*, **56**, 191–197.
24. Xu,Q. and Lee,C. (2003) Discovery of novel splice forms and functional analysis of cancer-specific alternative splicing in human expressed sequences. *Nucleic Acids Res.*, **31**, 5635–5643.
25. Bubinek,J.L. and Driscoll,D.M. (2007) Altered RNA Binding Activity Underlies Abnormal Thyroid Hormone Metabolism Linked to a Mutation in Selenocysteine Insertion Sequence-binding Protein 2. *J. Biol. Chem.*, **282**, 34653–34662.
26. Mount,S.M. (1982) A catalogue of splice junction sequences. *Nucleic Acids Res.*, **10**, 459–472.
27. Castellano,S., Lobanov,A.V., Chapple,C., Novoselov,S.V., Albrecht,M., Hua,D., Lescure,A., Lengauer,T., Krol,A., Gladyshev,V.N. *et al.* (2005) Diversity and functional plasticity of eukaryotic selenoproteins: identification and characterization of the SelJ family. *Proc. Natl Acad. Sci. USA*, **102**, 16188–16193.
28. Kryukov,G.V. and Gladyshev,V.N. (2004) The prokaryotic selenoproteome. *EMBO Rep.*, **5**, 538–543.
29. Zhang,Y., Fomenko,D.E. and Gladyshev,V.N. (2005) The microbial selenoproteome of the Sargasso Sea. *Genome Biol.*, **6**, R37.
30. Singh,N.K., Singh,N.N., Androphy,E.J. and Singh,R.N. (2006) Splicing of a critical exon of human Survival Motor Neuron is regulated by a unique silencer element located in the last intron. *Mol. Cell Biol.*, **26**, 1333–1346.
31. Sazani,P. and Kole,R. (2003) Therapeutic potential of antisense oligonucleotides as modulators of alternative splicing. *J. Clin. Invest.*, **112**, 481–486.
32. Caban,K., Kinzy,S.A. and Copeland,P.R. (2007) The L7Ae RNA binding motif is a multifunctional domain required for the ribosome-dependent Sec incorporation activity of Sec insertion sequence binding protein 2. *Mol. Cell Biol.*, **27**, 6350–6360.
33. Jean,S., Bideau,C., Bellon,L., Halimi,G., De Meo,M., Orsiere,T., Dumenil,G., Berge-Lefranc,J.L. and Botta,A. (2001) The expression of genes induced in melanocytes by exposure to 365-nm UVA: study

by cDNA arrays and real-time quantitative RT-PCR. *Biochim. Biophys. Acta*, **1522**, 89–96.
34. Kryukov,G.V., Kryukov,V.M. and Gladyshev,V.N. (1999) New mammalian selenocysteine-containing proteins identified with an algorithm that searches for selenocysteine insertion sequence elements. *J. Biol. Chem.*, **274**, 33888–33897.
35. Marc,P., Margeot,A., Devaux,F., Blugeon,C., Corral-Debrinski,M. and Jacq,C. (2002) Genome-wide analysis of mRNAs targeted to yeast mitochondria. *EMBO Rep.*, **3**, 159–164.
36. Margeot,A., Garcia,M., Wang,W., Tetaud,E., di Rago,J.P. and Jacq,C. (2005) Why are many mRNAs translated to the vicinity of mitochondria: a role in protein complex assembly? *Gene*, **354**, 64–71.
37. Sylvestre,J., Margeot,A., Jacq,C., Dujardin,G. and Corral-Debrinski,M. (2003) The role of the 3′ untranslated region in mRNA sorting to the vicinity of mitochondria is conserved from yeast to human cells. *Mol. Biol. Cell*, **14**, 3848–3856.
38. Miranda-Vizuete,A., Damdimopoulos,A.E., Pedrajas,J.R., Gustafsson,J.A. and Spyrou,G. (1999) Human mitochondrial thioredoxin reductase cDNA cloning, expression and genomic organization. *Eur. J. Biochem.*, **261**, 405–412.
39. Pushpa-Rekha,T.R., Burdsall,A.L., Oleksa,L.M., Chisolm,G.M. and Driscoll,D.M. (1995) Rat phospholipid-hydroperoxide glutathione peroxidase. cDNA cloning and identification of multiple transcription and translation start sites. *J. Biol. Chem.*, **270**, 26993–26999.
40. Esworthy,R.S., Ho,Y.S. and Chu,F.F. (1997) The Gpx1 gene encodes mitochondrial glutathione peroxidase in the mouse liver. *Arch. Biochem. Biophys.*, **340**, 59–63.
41. Ma,Y. and Taylor,S.S. (2008) A Molecular Switch for Targeting between Endoplasmic Reticulum (ER) and Mitochondria: conversion of a mitochondria-targeting element into an ER-targeting signal inIN DAKAP1. *J. Biol. Chem.*, **283**, 11743–11751.
42. de Jesus,L.A., Hoffmann,P.R., Michaud,T., Forry,E.P., Small-Howard,A., Stillwell,R.J., Morozova,N., Harney,J.W. and Berry,M.J. (2006) Nuclear assembly of UGA decoding complexes on selenoprotein mRNAs: a mechanism for eluding nonsense-mediated decay? *Mol. Cell Biol.*, **26**, 1795–1805.
43. Squires,J.E., Stoytchev,I., Forry,E.P. and Berry,M.J. (2007) SBP2 binding affinity is a major determinant in differential selenoprotein mRNA translation and sensitivity to nonsense-mediated decay. *Mol. Cell Biol.*, **27**, 7848–7855.
44. Kryukov,G.V., Castellano,S., Novoselov,S.V., Lobanov,A.V., Zehtab,O., Guigo,R. and Gladyshev,V.N. (2003) Characterization of mammalian selenoproteomes. *Science*, **300**, 1439–1443.
45. Kim,V.N. and Nam,J.W. (2006) Genomics of microRNA. *Trends Genet.*, **22**, 165–173.